

Design of Piezoelectric Energy Harvester with Controlled and Regulated Output Voltage: Simulation Study

SUNITHAMANI.S¹ LAKSHMI.P², EBA FLORA.E³
 Department of EEE, College of Engineering, Guindy,
 Anna University, Chennai, INDIA.

¹sunithabavi@gmail.com, ²p_lakshmi@annauniv.edu, ³ebenflora@gmail.com.

Abstract: Piezoelectric energy harvester converts mechanical vibration into electrical energy via piezoelectric effect. Geometry of the energy harvester play vital role in scavenging energy from vibration. Therefore six different geometries are simulated. The voltage produced by the energy harvester has to be either stored in a storage unit like capacitor/battery or it should be transferred. Voltage produced by energy harvester is ac and it is rectified and then regulated using buck converter. In a buck converter application, it is desired to obtain a constant output voltage $v(t) = V$, in spite of disturbances in $v_g(t)$, $i_{load}(t)$ and in the converter circuit parameters. To obtain constant output voltage a compensator device of the system is designed by using series compensation. The stability of the closed-loop Buck system has been greatly improved by using series compensator.

Keywords: Piezoelectric energy harvester, Finite element analysis, different cantilever structures, compensator.

1 Introduction

With recent growth in the development of low-power electronic devices such as microelectronics and wireless sensor nodes, as well as the global interest in the concept of “green” engineering, the topic of energy harvesting has received much attention in the past decade. The use of batteries, however, presents several drawbacks including the cost of battery replacement as well as limitations imposed by the need of convenient access to the device for battery replacement purposes. By scavenging ambient energy surrounding an electronic device, energy harvesting solutions have the ability to provide permanent power sources that do not require periodic replacement. Adnan Harb discussed about the advances in energy harvesting technique from vibration, thermal, and RF sources as well as power management techniques.

The geometry of a piezoelectric cantilever beam will greatly affects its vibration energy harvesting ability. The best piezoelectric device harvests about 5% of the available power. This indicates that there are still enormous resources to design more efficient harvesters. Frank Goldschmidtboeing and Peter Woias discussed about the analysis of different beam shapes for piezoelectric energy harvesters. It turns out that triangular-shaped with rectangular cross section beams are more effective than rectangular-shaped cantilever with rectangular cross section in terms of curvature homogeneity independent of the proof mass. JiaWen Xu et al discussed about the piezoelectric cantilever generator with a right-angle structure. The auxiliary beam length is varied to get optimal power. Analysis shows that the extended part provides a large torque to the main beam, which can dramatically smoothen the

strain distribution of the main beam and has the ability to scavenge more voltage. M. Guizzetti et al discussed about the techniques to get maximum electrical energy by varying the thickness of piezoelectric layer. Finite Element Model simulations have been used in order to optimize the piezoelectric layer thickness. Suyog N Jagtap and Roy Paily discussed optimization techniques by varying thickness, length and width of metal and ZnO to get maximum displacement and voltage. They have proved that the energy harvester has the ability to scavenge more energy when the length, width and thickness of the cantilever are optimised.

Xu-rui Chen et al discussed about the feasibility of taking PZT circular diaphragm as an energy harvester and optimized the contacting part between the mass and the piezoelectric disc to get maximum output voltage and power. By optimizing the contacting part ratio, the energy harvester's efficiency is improved. Z.S.Chen et al discussed about the strain formulation of rectangular, trapezoidal and triangular piezoelectric cantilevers. Simulation and experiment results demonstrate that under the loading conditions, triangular cantilever beams can improve the strain distribution and generate more voltage than trapezoidal and rectangular. The cantilever beams are mostly in rectangular cross section. Eba Flora et al proved that the cantilevers with trapezoidal cross section produced more voltage. Andreza Tangerino Mineto et al discussed about placing the piezoelectric material only at the fixed end because strain is maximum at the fixed end. Since strain is directly proportional to the voltage produced, the energy harvester can produce more voltage if piezoelectric material is placed only at the fixed end. Nechibvute Action et al discussed about the different piezoelectric materials for energy harvester and the voltage produced by them.

A comparative study of the traditional PZT ceramics and new single crystals is critical in selecting the best material and optimization of transducer design for applications such as conversion of ambient vibrations into useful electrical energy. In this paper a simulation study is performed to prove that the new single crystal can harvest more voltage compared to traditional piezoelectric materials. Ahmadreza Tabesh and Luc G. Fréchet discussed about energy harvester, its rectifying methods and getting regulated output voltage using step down converter and its control. Two types of rectifying circuit is discussed one is the bridge rectifier and the other is the voltage doubler. S.Sunithamani et al optimized the length of the piezoelectric layer to enhance the performance of the energy harvester. S.Sunithamani et al studied on performance of MEMS piezoelectric energy harvester with optimized substrate to piezoelectric thickness ratio.

In this paper Six different cantilever structures namely Rectangular Cantilever with Rectangular Cross Section (RCRC), Rectangular Cantilever with Trapezoidal Cross Section (RCTAC), Trapezoidal Cantilever with Rectangular Cross Section (TACRC), Trapezoidal Cantilever with Trapezoidal Cross Section (TACTAC), Triangular Cantilever with Rectangular Cross Section (TRCRC) and Triangular Cantilever with Trapezoidal Cross Section (TRCTAC) are designed and shown in Figure 1. These geometries are simulated using the software COMSOL Multiphysics. Finite element analysis and frequency analysis are carried out to find out the best energy harvester geometry. Then the output voltage is rectified, regulated and controlled for further usage of regulated voltage by electronic devices like laptops, which use approximately 20V.

2 Design and Geometry modeling in COMSOL Multiphysics

Six different geometries made of single crystal PMN 32 as piezoelectric layer and stainless steel as the substrate are modelled using the software COMSOL Multiphysics.

The output voltage produced by the energy harvester is directly proportional to strain. Strain is maximum at the fixed end of the cantilever. So it is sufficient to place the piezoelectric ceramics at the fixed end. In order to get maximum output voltage, the thickness of the substrate layer should be less than the thickness of the piezoelectric layer. The length and thickness of the substrate layer is 27000 μm and 200 μm . The length and thickness of the single crystal PMN32 layer is shown in Table 1. A point load of 0.2 N is applied at the free end of the cantilever.

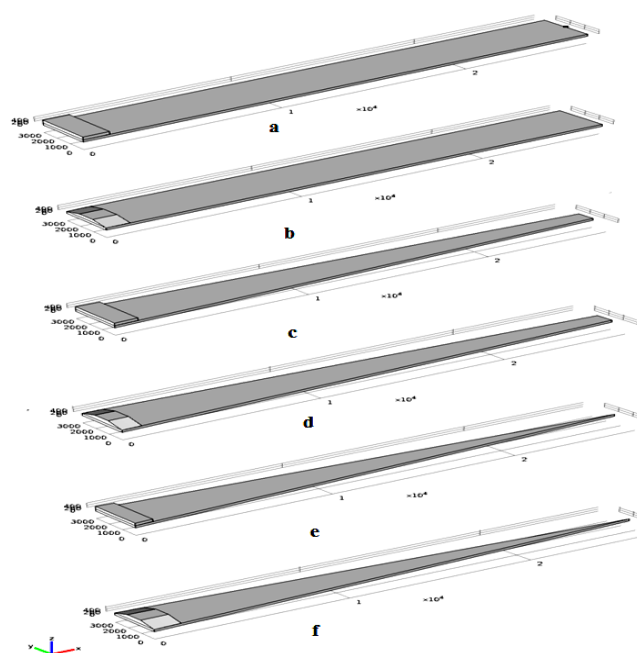


Figure 1 Six different Structures of cantilever.
a)RCRC b)RCTAC c)TACRC d)TACTAC e)TRCRC
f) TRCTAC

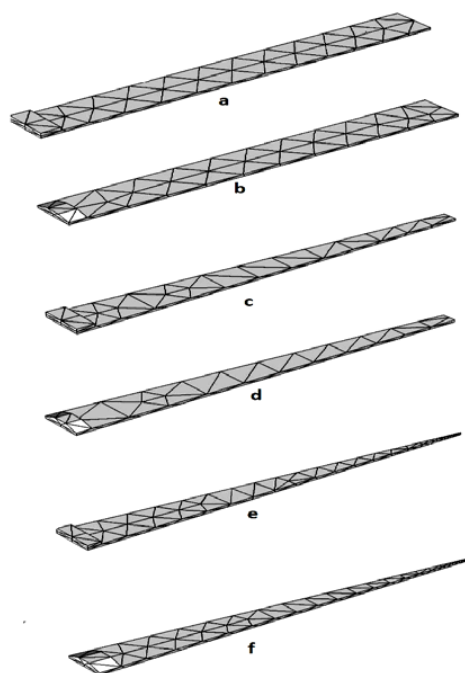


Figure 2 Finite Element Model of Geometries (a) RCRC (b) RCTAC (c) TACRC (d) TACTAC (e) TRCRC (f) TRCTAC.

Table 1. Dimensions of single crystal PMN32 layer for six different cantilever structures

Structures	Thickness (μm)	Length (μm)
RCRC	260	1300
RCTAC	260	1200
TACRC	240	1200
TACTAC	340	1000
TRCRC	230	900
TRCTAC	340	1400

2.1 Finite Element Analysis

In order to get accurate and convenient results, finite element analysis is carried out for all the six geometries. It is used to study the moment of inertia and strain. The finite element models of all the six geometries are shown in Figure 2.

The generated output voltage is directly proportional to strain. The strain ε of a piezoelectric cantilever vibrator at the distance of x is given by

$$\varepsilon (x, z) = -\frac{M(x)z}{E \times I} \quad (1)$$

Where $M(x)$ is the bending moment of a piezoelectric cantilever vibrator at the distance of x , z is the deformation, E the Young's modulus of the material and I the moment of inertia. From Eq. (1), it can be inferred that the strain is inversely proportional to the moment of inertia otherwise output voltage is also inversely proportional to moment of inertia.

2.2 Frequency Analysis

Piezoelectric harvesters are very efficient when they are driven in resonant frequencies. Therefore they suit well for applications with known excitation frequency. Frequency analysis is carried out for all the six geometries with frequency ranging from 1 Hz to 1KHz using the physics frequency analysis, in COMSOL Multiphysics and the output voltage produced at their respective resonant frequencies are found out. The resonant frequencies of the six harvesters and the output

voltage produced at their resonant frequency are shown in Figure 3.

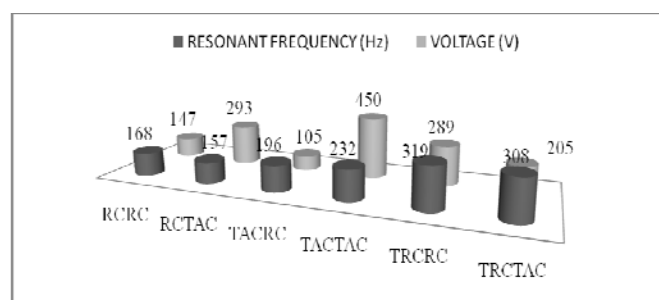


Figure 3 Resonant Frequency (Hz) of the Six Harvesters and the Output voltage (V) Produced by the Harvesters at their Resonant Frequencies

2.3 Switching Circuit for Piezoelectric Energy Harvester

The piezoelectric voltage can vary in a wide range due to the variation of mechanical vibration excitations, while on the other hand electronic devices require a constant regulated voltage. To retain maximum power extraction, one of the method is to adjust the rectified voltage with respect to the piezoelectric open-circuit voltage (V_{oc}) by using a dc-dc power converter. Step-down (buck) converter is used as switching circuit, since the voltage (V_{oc}) is often higher than the voltage of the battery. Using series compensation, a compensator device of the system is designed. The stability of the closed-loop (Buck) system has greatly improved.

The output voltage produced by the energy harvester is a.c, so it is rectified using a full wave rectifier. Rectifier is followed by a filter capacitor and it is used to reduce the fluctuations of the filter voltage. The output voltage of the energy harvester is used as an input to the rectifier and the switching circuit is simulated using the software MATLAB/Simulink. The circuit diagram showing piezoelectric energy harvester and all other components are shown in figure 4. The switching circuit which is a buck converter is shown in figure 5.

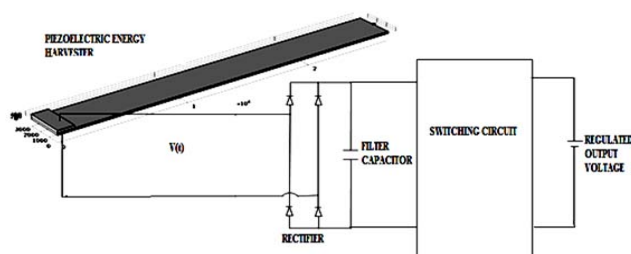


Figure 4 Proposed Circuitry through a Simplified Circuit Diagram.

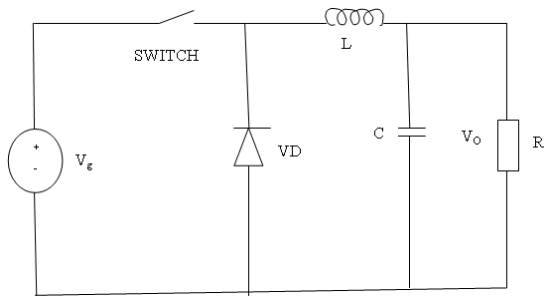


Figure 5 Buck Converter

In figure 5 V_g is the voltage across the filter capacitor. The output ripple current is 0.05 A, the output ripple voltage is 0.03 V, resistance R is 20 Ω and the frequency of PWM is fixed as 40 KHz. Based on these data the L, C and the duty cycle D values are calculated using the following equations.

$$\text{Duty cycle } D = \frac{V_o}{V_g} = \frac{t_{ON}}{T_s} \quad (2)$$

Output ripple current

$$\Delta i = \frac{V_g}{Lf} D (1 - D) \quad (3)$$

Output ripple voltage

$$\Delta v_o = \frac{V_o (1 - D)}{8 C L f^2} \quad (4)$$

The input voltage to the converter V_g , output voltage of the converter V_o , duty cycle D, inductance L and capacitance C for the six geometries are calculated and the values are tabulated in Table 2.

Table 2. Buck Converter Component Values

Structure	Input Voltage To The Converter V_g (V)	Output Voltage Of The Converter V_o (V)	Duty Cycle D	Inductance L (mH)	Capacitance C (μ F)
RCRC	147	20	0.14	9	5
RCTAC	293	20	0.07	9	5
TACRC	105	20	0.2	8	5
TACTAC	450	20	0.045	9	6
TRCRC	289	20	0.07	9	5
TRCTAC	205	20	0.1	9	5

The piezoelectric energy harvester output voltage, rectifier output voltage and regulated output voltage is shown in figure from 6 to 11.

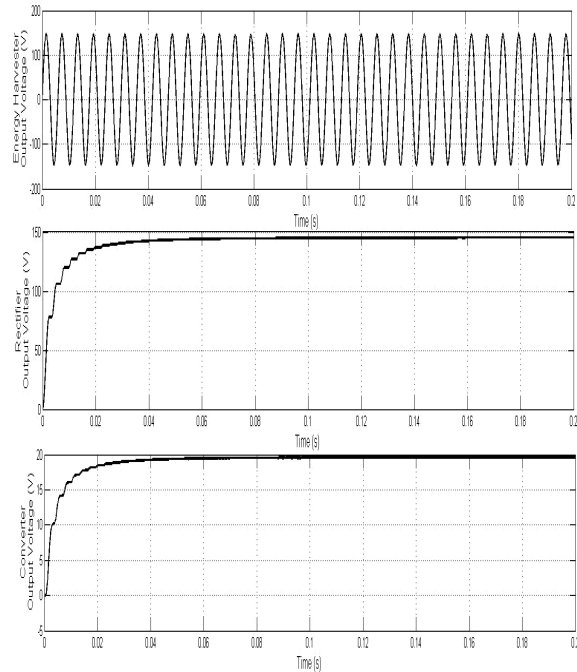


Figure 6 Piezoelectric Energy Harvesters, Rectifier and Regulated Output Voltage For the Geometry RCRC

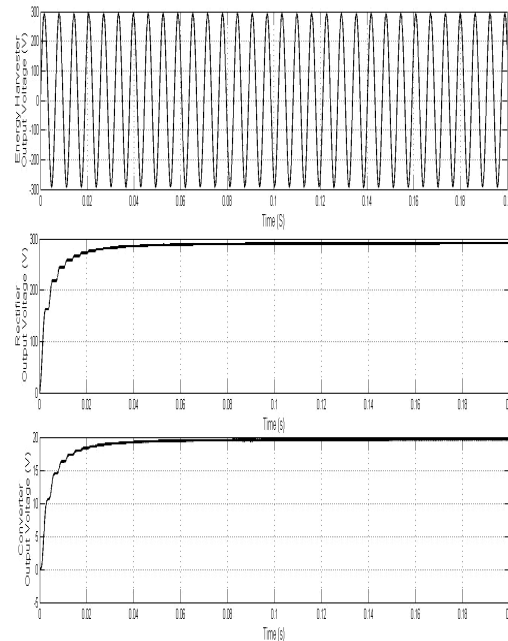


Figure 7 Piezoelectric Energy Harvester, Rectifier and Regulated Output Voltage For the Geometry RCTAC.

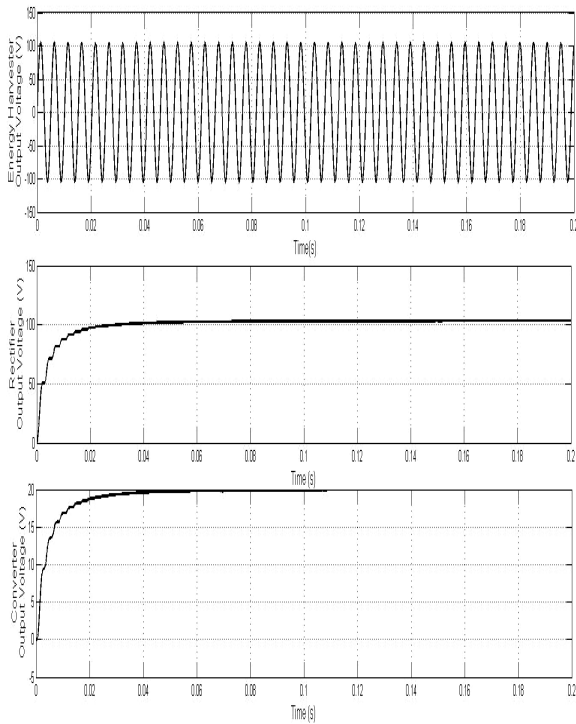


Figure 8 Piezoelectric Energy Harvesters, Rectifier and Regulated Output Voltage For the Geometry TACRC

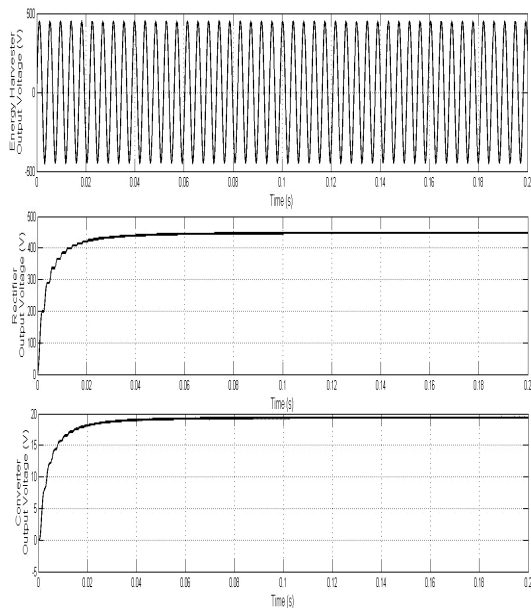


Figure 9 Piezoelectric Energy Harvester, Rectifier and Regulated Output Voltage For the Geometry TACTAC

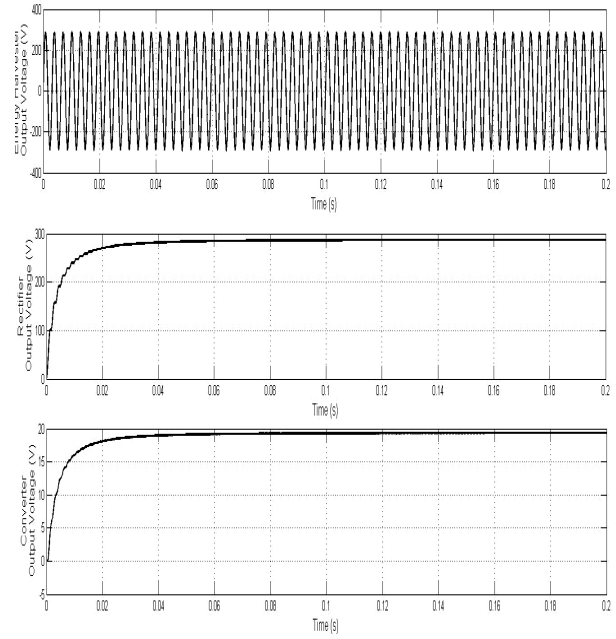


Figure 10 Piezoelectric Energy Harvester, Rectifier and Regulated Output Voltage For the Geometry TRCRC

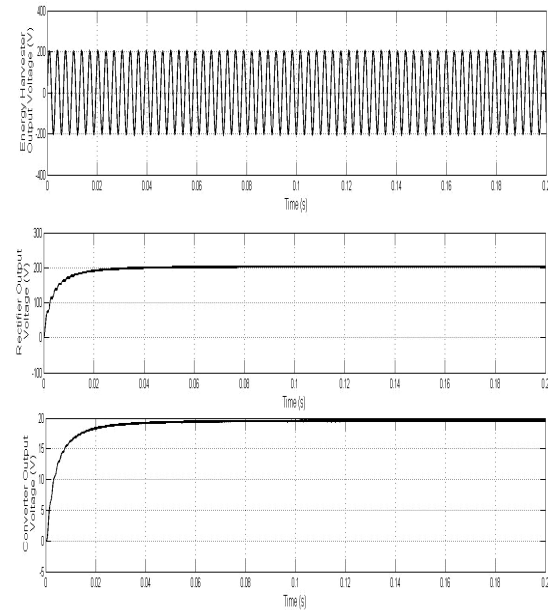


Figure 11 Piezoelectric Energy Harvester, Rectifier and Regulated Output Voltage For the Geometry TRCTAC.

From the above figures it is seen that the rectified output voltage for each structure has various voltage values and are regulated to 20V by using a buck converter.

2.4 System Modeling

State-space averaging is a powerful way to treat analysis and control problems for variable structure systems. State-space averaging method was proven to be the first order approximation of averaging method. The working state of Buck converter is described as two electric circuits.

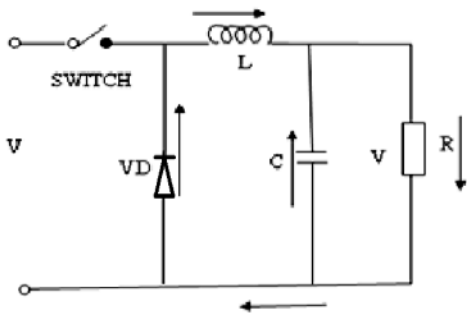


Figure 12. Switch in open position

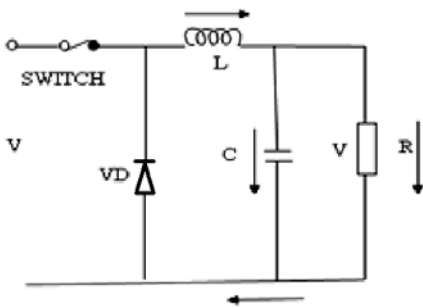


Figure 13. Switch in close position

While the switch is in open position, the inductor voltage, capacitor current, and converter input current are

$$L \frac{di_L}{dt} + v_c = v_g \quad (5)$$

$$C \frac{dv_c}{dt} + \frac{v_c}{R} = i_L \quad (6)$$

$$i_g - i_L \quad (7)$$

$$v_o = v_c \quad (8)$$

These equations can be written in the following state space form

$$\dot{x} = \begin{bmatrix} 0 & -1/L \\ 1/C & -1/RC \end{bmatrix} \begin{bmatrix} i_L \\ v_c \end{bmatrix} + \begin{bmatrix} 1/L \\ 0 \end{bmatrix} v_g \quad (9)$$

$$y = \begin{bmatrix} v_o \\ i_g \end{bmatrix} = \begin{bmatrix} 0 & 1 \\ 1 & 0 \end{bmatrix} \begin{bmatrix} i_L \\ v_c \end{bmatrix} + \begin{bmatrix} 0 \\ 0 \end{bmatrix} v_g \quad (10)$$

The state equation matrices are as follows

$$A_1 = \begin{bmatrix} 0 & -1/L \\ 1/C & -1/RC \end{bmatrix}, B_1 = \begin{bmatrix} 1/L \\ 0 \end{bmatrix}, C_1 = \begin{bmatrix} 0 & 1 \\ 1 & 0 \end{bmatrix}, E_1 = \begin{bmatrix} 0 \\ 0 \end{bmatrix}$$

With the switch in close position, for this subinterval, the inductor current, capacitor voltage, and converter input current are given by

$$L \frac{di_L}{dt} + v_c = 0 \quad (11)$$

$$C \frac{dv_c}{dt} + \frac{v_c}{R} = i_L \quad (12)$$

$$i_g = 0 \quad (13)$$

$$v_o = v_c \quad (14)$$

When written in state-space form, these equations become

$$\dot{x} = \begin{bmatrix} 0 & -1/L \\ 1/C & -1/RC \end{bmatrix} \begin{bmatrix} i_L \\ v_c \end{bmatrix} + \begin{bmatrix} 0 \\ 0 \end{bmatrix} v_g \quad (15)$$

$$y = \begin{bmatrix} v_o \\ i_g \end{bmatrix} = \begin{bmatrix} 0 & 1 \\ 0 & 0 \end{bmatrix} \begin{bmatrix} i_L \\ v_c \end{bmatrix} + \begin{bmatrix} 0 \\ 0 \end{bmatrix} v_g \quad (16)$$

The state equation matrices are as follows

$$A_2 = \begin{bmatrix} 0 & -1/L \\ 1/C & -1/RC \end{bmatrix}, B_2 = \begin{bmatrix} 0 \\ 0 \end{bmatrix}, C_2 = \begin{bmatrix} 0 & 1 \\ 0 & 0 \end{bmatrix}, E_2 = \begin{bmatrix} 0 \\ 0 \end{bmatrix}, D' = 1 - D$$

The state space averaged model that describes the converter in equilibrium is

$$0 = AX + BU \quad (17)$$

$$Y = CX + EU \quad (18)$$

The next step is to evaluate the state-space averaged equilibrium equations. The averaged matrices A, B, C and E is

$$A = DA_1 + D'A_2 = A_1 = A_2 \quad (19)$$

$$B = DB_1 + D'B_2 = \begin{bmatrix} D/L \\ 0 \end{bmatrix} \quad (20)$$

$$C = DC_1 + D'C_2 = \begin{bmatrix} 0 & 1 \\ D & 0 \end{bmatrix} \quad (21)$$

$$E = DE_1 + D'E_2 = \begin{bmatrix} 0 \\ 0 \end{bmatrix} \quad (22)$$

The small-signal AC model described by state equations is as follows

$$\frac{d\hat{d}(t)}{dt} = A\hat{x}(t) + B\hat{u}(t) + [(A_1 - A_2)X + (B_1 - B_2)U]\hat{d}(t) \quad (23)$$

$$\hat{y}(t) = C\hat{x}(t) + E\hat{u}(t) + [(C_1 - C_2)X + (E_1 - E_2)U]\hat{d}(t) \quad (24)$$

The small-signal AC state therefore become

$$\frac{d}{dt} \begin{bmatrix} \hat{i}_L(t) \\ \hat{v}_c(t) \end{bmatrix} = \begin{bmatrix} 0 & -1/L \\ 1/C & -1/RC \end{bmatrix} \begin{bmatrix} \hat{i}_L(t) \\ \hat{v}_c(t) \end{bmatrix} + \begin{bmatrix} D/L \\ 0 \end{bmatrix} \hat{v}_g(t) + \begin{bmatrix} 1/L \\ 0 \end{bmatrix} v_g \hat{d}(t) \quad (25)$$

$$\hat{y}(t) = \begin{bmatrix} \hat{v}_o(t) \\ \hat{i}_g(t) \end{bmatrix} = \begin{bmatrix} 0 & 1 \\ D & 0 \end{bmatrix} \begin{bmatrix} \hat{i}_L(t) \\ \hat{v}_c(t) \end{bmatrix} + \begin{bmatrix} 0 & 0 \\ 1 & 0 \end{bmatrix} \begin{bmatrix} L \\ DV_g \end{bmatrix} \hat{d}(t) \quad (26)$$

By writing the equations (25) and (26) in scalar form and taking Laplace transform the equation becomes

$$Ls\hat{i}_L(s) = -\hat{v}_c(s) + D\hat{v}_g(s) + v_g \hat{d}(s) \quad (27)$$

$$C\hat{v}_c(s) = \hat{i}_L(s) - \hat{v}_c(s)/R \quad (28)$$

$$\hat{v}_o(s) = \hat{v}_c(s) \quad (29)$$

$$\hat{i}_g(s) = D\hat{i}_L(s) + I_L \hat{d}(s) \quad (30)$$

By simplifying the above equations (27) to (30)

$$\hat{v}_o(s) = \hat{v}_c(s) = \frac{D}{LCs^2 + \frac{L}{R}s + 1} \hat{v}_g(s) + \frac{v_g}{LCs^2 + \frac{L}{R}s + 1} \hat{d}(s) \quad (31)$$

$$G_{vg}(s) = \frac{\hat{v}_o(s)}{\hat{v}_g(s)} / \hat{d}(s) = 0 = \frac{D}{LCs^2 + \frac{L}{R}s + 1} \quad (32)$$

$$G_{vd}(s) = \frac{\hat{v}_o(s)}{\hat{d}(s)} / \hat{v}_g(s) = 0 = \frac{v_g}{LCs^2 + \frac{L}{R}s + 1} \quad (33)$$

$G_{vd}(s)$ is the converter control-to-output transfer function. $G_{vg}(s)$ is the converter input line-to-output transfer function. The transfer function of the pulse-width modulator is

$$G_{dc}(s) = \frac{\hat{d}(s)}{\hat{v}_c(s)} = \frac{1}{v_m} \quad (34)$$

v_m is the maximum of the saw tooth wave of the pulse widthmodulator.

2.5 Compensator Design

In buck converter, the output voltage $v(t)$ is a function of the input line voltage $v_g(t)$, the duty cycle $d(t)$, and the load current $i_{load}(t)$, as well as the converter circuit element values. In a buck converter application, it is desired to obtain a constant output voltage $v(t) = V$, in spite of disturbances in $v_g(t)$, $i_{load}(t)$ and in the converter circuit parameters. A typical power supply specification is that the output voltage must remain within a specified range. It is desired that essentially all of this distribution fall within the specified range; however, this is not practical to achieve without the use of negative feedback. The idea behind the use of negative feedback is to build a

circuit that automatically adjusts the duty cycle as necessary, to obtain the desired output voltage with high accuracy, regardless of disturbances in $v_g(t)$ or $i_{load}(t)$ or variations in component values. A block diagram of a feedback system is shown in figure 14.

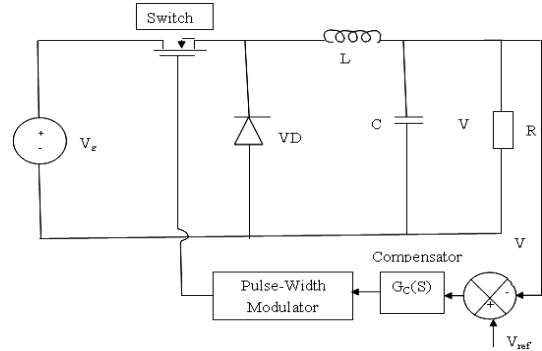


Figure 14 Buck Converter with Feedback.

Table 3 Open loop Transfer Function of buck converter

STRUCTURE	TRANSFER FUNCTION
RCRC	$\frac{653.33e6}{s^2 + 10e3s + 22.2e6}$
RCTAC	$\frac{61.7e6}{s^2 + 10e3s + 21e6}$
TACRC	$\frac{26.25e6}{s^2 + 10e3s + 25e6}$
TACTAC	$\frac{83.3e6}{s^2 + 8.3e3s + 18.5e6}$
TRCRC	$\frac{64.2e6}{s^2 + 10e3s + 22e6}$
TRCTAC	$\frac{45.5e6}{s^2 + 10e3s + 22e6}$

The open-loop transfer function of buck converter is

$$G_o(s) = G_{vd}(s)G_{dc}(s) = \frac{v_g}{LCs^2 + \frac{L}{R}s + 1} \frac{1}{v_m}$$

By substituting L, C, R and v_m values the open loop transfer function of the six geometries are shown in Table 3. As the electronic devices require constant input voltage, a compensator is designed to get a constant output voltage from the bulk converter. The compensator is shown in figure 15.

The crossover frequency of feedback system with compensator should be equal to $2\pi f_s / 10 = 25.133$ KHz.

The compensator transfer functions of six geometries are tabulated in Table 4.

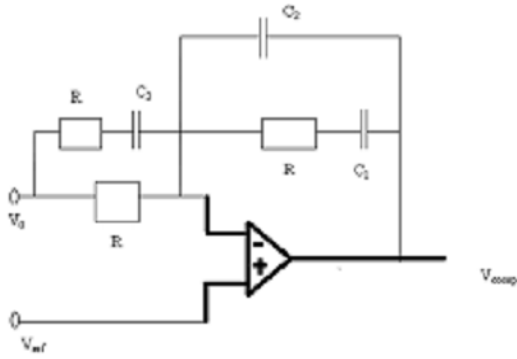


Figure 15 Compensator.

Table 4. Compensator Transfer Function of six geometries

STRUCTURE	COMPENSATOR TRANSFER FUNCTION
RCRC	$\frac{2.6e3s^2 + 18.9e6s + 3e11}{s^3 + 2.9e3s^2 + 3.4e6s}$
RCTAC	$\frac{250e3s^2 + 1.24e9s + 1.5e12}{s^3 + 5e3s^2 + 625e6s}$
TACRC	$\frac{250e3s^2 + 1.24e9s + 1.5e12}{s^3 + 250.6e3s^2 + 250e6s}$
TACTAC	$\frac{254e3s^2 + 1.05e9s + 1e12}{s^3 + 250e3s^2 + 834e6s}$
TRCRC	$\frac{495e3s^2 + 1.9e9s + 1.5e12}{s^3 + 250.6e3s^2 + 625e6s}$
TRCTAC	$\frac{2.7e6s^2 + 7.4e9s + 1.5e12}{s^3 + 250.6e3s^2 + 625e6}$

3 Results and Discussions

By using the buck converter compensation technique, the voltage produced by the energy harvester is regulated to get constant output voltage which is directly used by the electronic devices. This is shown in figures from 16 to 21.

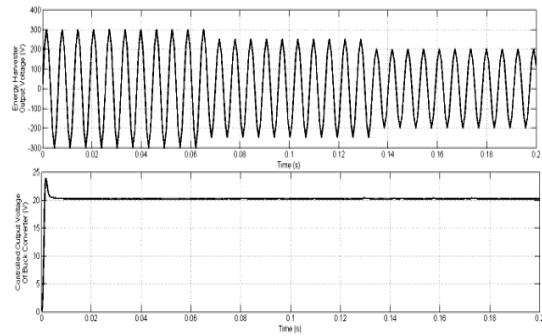


Figure 17 Buck Converter Output Voltage for Various Voltage Produced by the geometry RCTAC

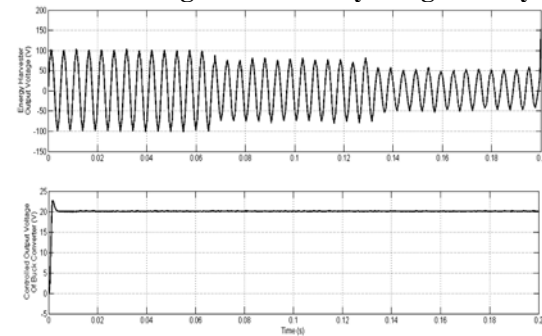


Figure 18 Buck Converter Output Voltage for Various Voltage Produced by the geometry TACRC

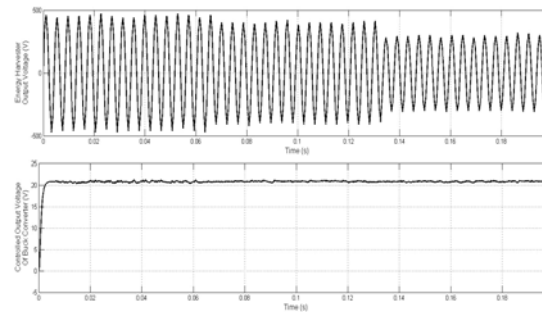


Figure 19 Buck Converter Output Voltage for Various Voltage Produced by the geometry TACTAC

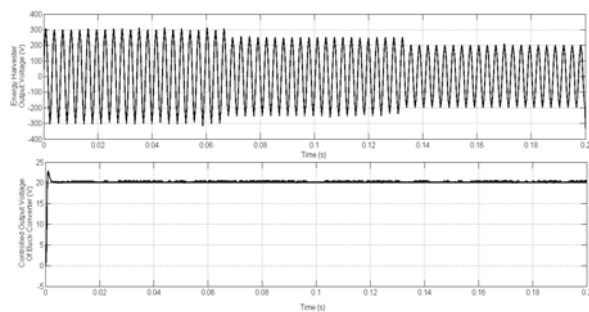


Figure 20 Buck Converter Output Voltage for Various Voltage Produced by the geometry TRCRC

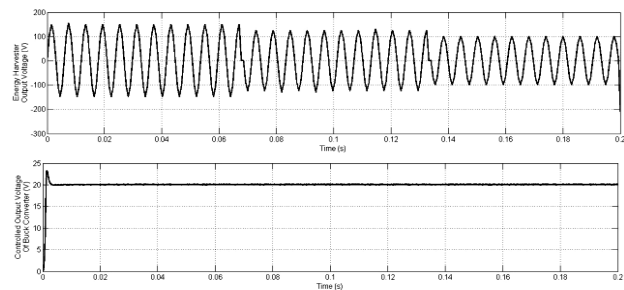


Figure 16 Buck Converter Output Voltage for Various Voltage Produced by the geometry RCRC

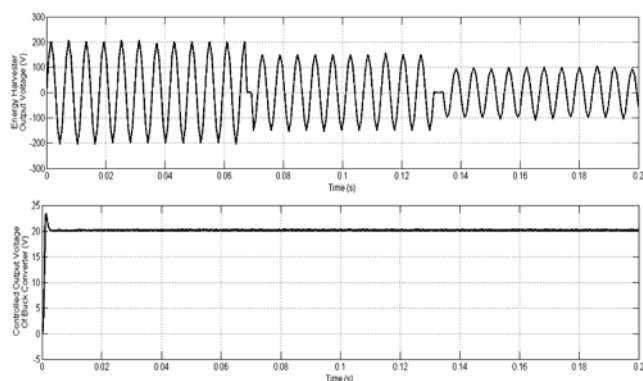


Figure 21 Buck Converter Output Voltage for Various Voltage Produced by the geometry TRCTAC

From the above figures it is seen that the energy harvester output voltage is varied from first resonance voltage to second, third resonance voltage value and so on. First resonance voltage is the highest voltage produced by energy harvester. In spite of these changes the output of the buck converter remains constant.

4 Conclusion

Six geometries RCRC, RCTAC, TACRC, TACTAC, TRCRC and TRCTAC are simulated. Frequency and finite element analysis are carried out to find the best geometry which can produce maximum voltage. Under the analysis it is concluded that the TACTAC produce more voltage compared to other geometries. The proposed circuit is useful for efficient energy conversion of vibrating piezoelectric generators with application to low power portable devices. An efficient piezoelectric energy harvester either increases the lifetime of the battery of a device or alternatively can be used as a long-life power supply for self-powered remote sensor nodes. With the help of compensator it is able to attend a constant regulated voltage in spite changes in voltage produced by the energy harvester. The proposed energy harvester with buck converter and compensator are used to power electronic devices like laptops, which use 20V voltage.

References

- [1] Adnan Harb, "Energy harvesting: State-of-the-art", *Journal of Renewable Energy*, Vol.36 (2011), pp 2641-2654
- [2] Frank Goldschmidtboeing., Peter Woias., "Characterization of different beam shapes for piezoelectric energy harvesting", *Journal of Microelectronics and Microengineering*, Vol.18, No.10, 2008.
- [3] Jia Wen Xu., Yong Bing Liu., Wei Wei Shao and Zhihua Feng., "Optimization of a right-angle piezoelectric cantilever using auxiliary beams with different stiffness levels for vibration energy harvesting", *Journal of Smart Materials and Structures*, Vol.21, no.6, pp 1-13, 2012.
- [4] Guizzetti, M., Ferrari, V., Marioli, D., Zawada, T., "Thickness Optimization of a piezoelectric converter for Energy Harvesting", *COMSOL Conference Milan*, 2009.
- [5] Suyog N Jagtap., Roy Paily., "Geometry Optimization of a MEMS-based Energy Harvesting Device", *Proceeding of the 2011 IEEE Students' Technology Symposium*, pp 1-5, 2011.
- [6] Xu-ruiChen., Tong-qingYang., Wei Wang., XiYao., "Vibration energy harvesting with a clamped piezoelectric circular diaphragm", *Journal of Ceramic International*, Vol. 38 Supplement 1, pp.271-274, 2012.
- [7] Z. S. Chen, Y. M. Yang and G. Q. Deng, (2009) "Analytical and Experimental Study on Vibration Energy Harvesting Behaviors of Piezoelectric Cantilevers with Different Geometries" *International Conference on Sustainable Power Generation and Supply*, 2009. SUPERGEN '09, pp 1-6.
- [8] Eba Flora.E, Lakshmi.P, Sunithamani.S," Simulation of MEMS Energy Harvester with Different Geometries and Different Cross Sections", *IEEE International Conference on Information and Communication Technologies (ICT 2013)*, pp 1067-1070.
- [9] Andreza Tangerino Mineto, Meire Pereira de Souza Braun, Hélio Aparecido Navarro, Paulo Sérgio Varoto, "Modeling Of A Cantilever Beam For Piezoelectric Energy Harvesting", *DINCON'10, 9th Brazilian conference on Dynamics and their Applications*, 2010.
- [10] Nechibvute Action., Chawanda Albert., Luhanga Pearson., "Finite Element Modeling of a Piezoelectric Composite Beam and Comparative Performance Study of Piezoelectric Materials for Voltage Generation" *ISRN Materials Science*, Volume 2012, Article ID 921361, pp 1-11, 2012.
- [11] Ahmadreza Tabesh., Luc G. Fréchet., "A Low-Power Stand-Alone Adaptive Circuit for Harvesting Energy From a Piezoelectric Micropower Generator", *IEEE Transactions On Industrial Electronics*, Vol. 57, No. 3, pp 840-849, 2010.
- [12] Sunithamani S, Lakshmi P, Eba Flora E (2013) "PZT length optimization of MEMS piezoelectric energy harvester with a non-traditional cross section: simulation study",

- Journal of Microsystem technologies. DOI 10.1007/s00542-013-1920-y.
- [13] Sunithamani S, Lakshmi P, (2014) “Simulation study on performance of MEMS piezoelectric energy harvester with optimized substrate to piezoelectric thickness ratio”, Journal of Microsystem technologies. DOI 10.1007/s00542-014-2226-4.